

Assessment of Wind Power Quality: Implementation of IEC61400-21 Procedures

A. Morales¹, X. Robe² and J.C. Maun¹

¹ Department of Electrical Engineering, CP 165/52

Université Libre de Bruxelles

Campus of Solbosch – 1050, Brussels (Belgium)

Phone/Fax number:+32 2 650 26 63/26 53, e-mail: amorales@ulb.ac.be, jcmaun@ulb.ac.be

² L' Air Liquide Luxembourg, S.A.

L-4801 Rodange (Luxembourg)

Phone/Fax number:+352 50 62 631/62 63 218, e-mail: Xavier.Robe@airliquide.com

Abstract. The purpose of this paper is to present the implementation of power quality procedures meeting the IEC 61400-21 standard. The system's architecture is detailed in the paper. An experimental laboratory setup which represents a fixed speed generation system is described. Measurements are carried out to test the proposed algorithm according to the measurement procedure for continuous operation of wind turbines. The assessment procedure is applied to investigate flicker emission.

Key words

Power quality, flicker, wind power.

1. Introduction

The IEC-61400-21 standard provides recommendations for preparing the measurements and assessment of power quality characteristics of wind turbines [1]. One important question is raised when trying to assess the power quality: who is responsible of flicker emissions? Generally, the influence of a wind turbine on the voltage quality of the grid depends not only on the turbine itself but also on the grid where it is connected. The European Wind Turbine Testing Procedure report and other publications have illustrated that the grid impedance angle and short circuit power have an important influence on the procedures proposed by the standard [2, 3]. We are then facing a very complex problem: how to measure the harmonic source impedance of a power network and to assess the emission level of a particular distorted generation [4].

2. IEC-61400-21: The measurement procedure

The measurement procedures described in the IEC-61400-21 standard are valid to test the power quality characteristic parameters for the full operational range

of a wind turbine, connected to a MV or HV network with fixed frequency within ± 1 Hz, sufficient active and reactive power regulation capabilities and sufficient load to absorb the wind power production. The *measurement procedures* are designed to be as non-site-specific as possible, so that power quality characteristics measured at for example a test site can be considered valid also at other sites. The standard specifies a method that uses current and voltage-time series, $i_m(t)$ and $u_m(t)$, measured at the wind turbine terminals distributed over the wind speed interval from cut-in to 15 m/s, to simulate the voltage fluctuations on a “fictitious” grid with no source of voltage fluctuations other than the wind turbine. This fictitious grid is presented in Fig. 1 by an ideal phase to neutral rated voltage source $u_o(t)$ with an appropriate apparent short-circuit power $S_{k, fic}$ and four grid impedance angles ψ_k ($30^\circ, 50^\circ, 70^\circ$ and 85°).

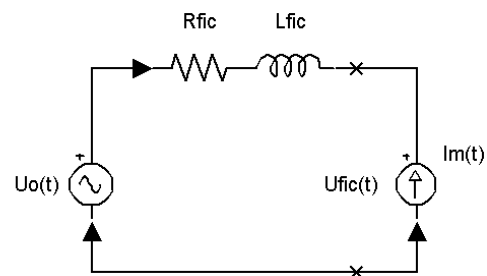


Fig. 1: Fictitious grid as proposed by IEC – 61400-21.

The wind turbine is represented by a current generator $i_m(t)$, which is the measured instantaneous value of the phase current. Thus, the fluctuating voltage that will be input to the voltage flicker algorithm in compliance with IEC-61000-4-15 to generate the flicker emission value $P_{st, fic}$ is given as:

$$u_{fic}(t) = u_0(t) + R_{fic} \cdot i_m(t) + L_{fic} \cdot \frac{d}{dt} i_m(t) \quad (1)$$

The fundamental voltage has to be determined from the measured voltage at the wind turbine terminals. Once this measurement and simulation procedure is done, flicker coefficients $c(\psi_k, v_a)$ are reported for continuous operation after normalization and weighting processes depending on the network impedance phase angle ψ_k and the annual average wind speed v_a . Flicker step factors $k_f(\psi_k)$ and voltage change factors $k_v(\psi_k)$ are generated together in the case of switching operations. These factors are normally measured and provided by manufacturers, who tend to overestimate them.

During the *assessment procedure*, in order to evaluate the power quality expected from a wind turbine when deployed at a specific site, the following equation applies at continuous operation:

$$P_{st} = P_n = c(\psi_k, v_a) \cdot \frac{S_n}{S_k} \quad (2)$$

where S_n is the rated apparent power of the wind turbine and S_k is the apparent short-circuit power at the PCC. Other equations are applied to assess the total contribution from several wind turbines. As reported in [3], flicker results are found to be strongly dependent on the grid impedance value, and the flicker summation from individual wind turbines gives too low total flicker values in case of limited supply strength.

3. Proposed implementation of the standard IEC-61400-21

The proposed system's architecture for implementation of power quality standards for wind turbines is detailed in this section. Only the measurement procedure is specified in the case of continuous operation. The implementation for switching operation is straightforward. Devices proposing basic power quality monitoring functions are already on the market meeting the IEC 61000 standards, but the IEC-61400-21 standard includes a simulation stage of voltage fluctuations on a fictitious grid.

This simulation is not very complicated except for the generation of the ideal voltage source $u_0(t)$ because it should fulfill the following properties [1]:

- 1) The ideal voltage should not display any fluctuations (zero flicker level).
- 2) It should have the same electrical angle $\alpha_m(t)$ as the fundamental of the measured voltage.

The ideal voltage is defined as:

$$u_0(t) = \sqrt{\frac{2}{3}} U_n \sin(\alpha_m(t)) = \sqrt{\frac{2}{3}} U_n \sin(2\pi \int_0^t f(t) dt + \alpha_0) \quad (3)$$

where U_n is the rms value of the nominal voltage of the grid, and the electrical angle $\alpha_m(t)$ of the measured voltage varies with frequency $f(t)$ within a measurement window. At the beginning of the time-series, the initial angle of the fundamental voltage is α_0 .

This ideal voltage angle calculation ensures that the phase angle between $u_{fic}(t)$ and $i_m(t)$ is correct, under the assumption that the voltage drop at the fictitious source impedance is much smaller than the ideal voltage amplitude. As illustrated in Figure 2, the error on the estimated phase angle increases with the source impedance value and angle. An appropriate apparent short circuit power of the fictitious grid $S_{k,fic}$ should be at least 50 times S_n , as recommended by the standard.

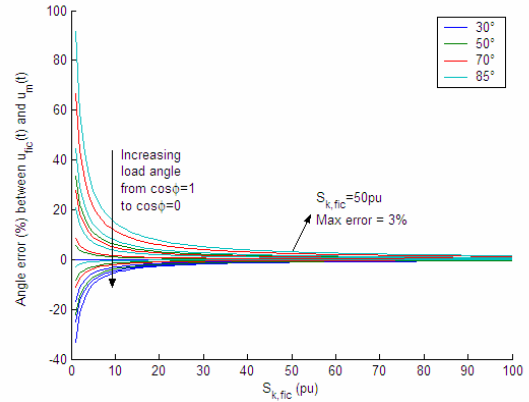


Fig. 2: Phase displacement of $u_{fic}(t)$ versus apparent short circuit power of the fictitious grid.

The obtained voltage time-series $u_{fic}(t)$ calculated using Equation (1) is then input to the flicker algorithm in compliance with IEC-61000-4-15 to give a flicker emission value $P_{st,fic}$ on the fictitious grid.

The angle of the ideal voltage is very important during the simulation phase since voltage fluctuations in $u_{fic}(t)$ are very sensitive to the angle value. If an error is committed on the fundamental voltage phase, the ideal voltage will be given by:

$$u_0(t) = \sqrt{\frac{2}{3}} U_n \sin(2\pi \int_0^t f(t) dt + \alpha_0 \pm \varepsilon_{\alpha_m}) \quad (4)$$

where ε_{α_m} represents the error or deviation from the measured voltage phase. Any deviation from the real electrical angle $\alpha_m(t)$ of the measured voltage has an impact on the amplitude of the calculated voltage $u_{fic}(t)$, what could bring the obtained simulated values outside the valid range of the flicker algorithm. This is illustrated with a numerical example in Figure 3, where the amplitude variation of the fictitious fundamental voltage $u_{fic}(t)$ expressed in per cent is plotted versus a variation of ε_{α_m} .

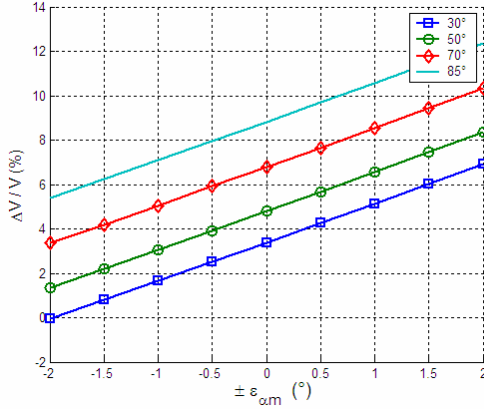


Fig. 3: Variation on $u_{fic}(t)$ relative amplitude versus deviations from the measured grid angle ($\epsilon_{\alpha m}$).

When implementing the full standard, special attention has to be paid to the calculation of the ideal fundamental voltage $u_0(t)$. Nowadays, the way to achieve the extraction of the fundamental frequency is by means of phase lock loop (PLL) equipment. The sampling frequency is calculated with a delay of 400 ms (20 cycles). The phase shift between windows due to this FFT error may be corrected and compensated. But the system frequency variations remain an important source of error when using present technology, and this is translated in erroneous phasor calculation.

Figure 4 illustrates the complex system proposed in this paper. It uses a constant sampling rate and thanks to a software resampling algorithm, measurements are rebuilt at a constant number of points per period. This algorithm is a combination of an interpolation (by an oversampling factor L) and a linear approximation. The main benefit is that the filter does not have to be computed for each window. It has been shown that its performances are good enough to meet the power quality standards, even for harmonics up to the 40th [5]. The main idea behind this design is, starting from a constant sampling rate at 10 or 20 kHz, to subdivide data into multiple streams at different sampling rates allowing flicker calculation and also performing accurate harmonic monitoring functions.

Accurate frequency tracking is one of the new improvements to the process. In this way, two phasors are obtained per window of $(40 \text{ ms} \pm \Delta t)$ length, with Δt the variable window length depending on the detected frequency. This allows a more accurate phasor calculation.

4. Algorithm description

A. Acquisition function

The *acquisition function* is built around one loop counting the number of data windows that have been acquired. One data window contains $C \cdot N$ points where C is the number of cycles per window and N is the desired number of points per cycle. (Selected values are $C = 2 \text{ cycles/window}$ and $N = 128 \text{ points/cycle}$.) The while-loop counts the number of samples in an output buffer. When this buffer is full, a new data window is acquired.

The number of cycles per window, parameter C , has been selected to obtain the highest accuracy when computing $u_0(t)$ from the resampled measured voltage $V_{new}(t)$. The voltage frequency is considered stationary within a window, and a window may be composed of ten, five or two cycles. Therefore, a shorter data window will provide the highest accuracy in frequency estimation and phasor calculation. Normally, standard power quality monitoring functions perform phasor calculations on a 10-cycle width basis.

B. Interpolation and linear approximation

The first element of this algorithm is the *low-pass FIR filter*. It is a 2-D array of coefficients. Each column of the filter allows computing one sample at $L f_s$ (f_s initial sampling frequency) avoiding multiplications by zero. The filter is built computing a Blackman window with the following parameters:

- L is the oversampling factor.
- M is the downsampling or decimation factor (set to 1 when using the linear approximation method).
- $ntaps$ is the number of rows in the matrix. It corresponds to the number of samples at f_s that will be used to compute one sample at $L f_s$.
- $cutoff$ is the cut-off frequency in per-unit (1 represents $f_s/2$).

Once the filter has been built, the next step is to compute the samples at $L f_s$ that surround the desired one. The two sample indexes are “ a ” and “ $a+1$ ”. The sample, at f_{sd} (desired new frequency, equal to $N f_v$ where f_v is the voltage frequency in the present window) is then given by the linear interpolation between “ a ” and “ $a+1$ ”.

When $C \cdot N$ points are in the output buffer, a 2-cycle window has been acquired, every counter should be reset and a new resampling frequency should be computed, ensuring the continuity between every 2-cycle window. First, FFT, rms, or other computations on the samples are made.

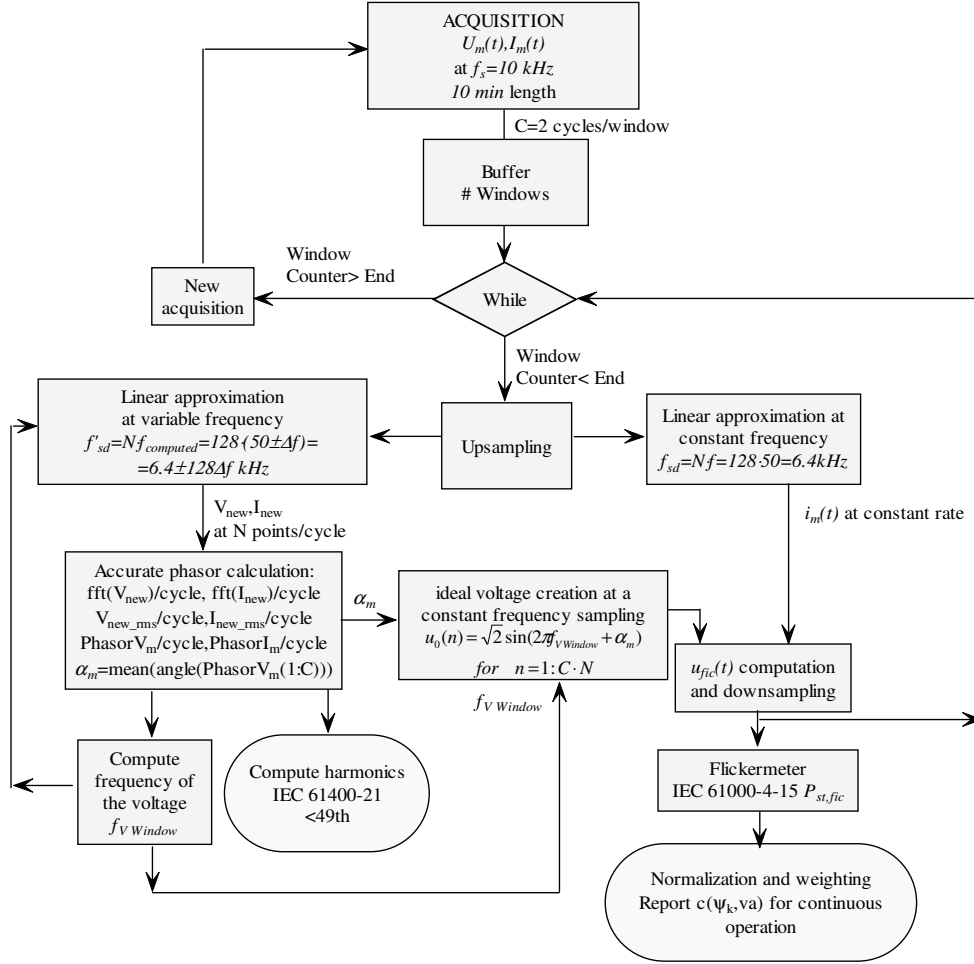


Fig. 4: Flowchart of the proposed algorithm.

C. Frequency computation

The estimated frequency is calculated in the data window using the DFT method. The first step is the extraction of the fundamental phasors by the DFT and phase correction (one for each cycle of the signal). The algorithm performs a linear regression, using the least square method, between these phases. The slope of the line is the frequency in the data window.

An additional feature of this algorithm is the rejection of the out-of-range measurements: if a phase is “too far” from the regression line, the program deletes it from the array of phases and recomputes a new regression line until all the remaining phases match it. If there are not enough remaining points, no frequency is computed.

D. Fast fourier transform

The FFT is computed on a fixed number of points per cycle after performing the signal resampling. The knowledge of fundamental values and phase displacement between measured voltage and current allows the computation of active and reactive power, and $\cos\phi$.

Harmonics are computed to the 49th component. The rms value of the h^{th} harmonic component, denoted by $I_{h(RMS)}$, is obtained in per cent on the rated current basis. Total harmonic distortion is given by:

$$THD(\%) = \frac{\sqrt{\sum_{h=2}^{49} I_{h(RMS)}^2}}{I_{1(RMS)}} \cdot 100 \quad (5)$$

where $I_{1(RMS)}$ is the rms value of the fundamental component.

E. Simulation of voltage fluctuations $u_{fic}(t)$

The ideal voltage $u_0(t)$ is obtained every two cycles at a variable or fixed sampling rate, according to:

$$u_0(n) = \sqrt{2} \sin(2\pi f_{V Window} n + \alpha_m) \quad n = 1, \dots, CN \quad (6)$$

When using a variable sampling rate, the measured current is also resampled and special care is taken to generate a variable time-step vector to perform the

derivative of the current in equation 1. The finite difference approximation is:

$$\frac{di(t)}{dt} = \frac{i_{n+1} - i_n}{\Delta t} \quad (7)$$

where Δt varies every two cycles due to the variable frequency sampling. The fictitious voltage is then obtained according to equation 1 at a variable sampling rate. Thus, interpolation and downsampling are performed for $u_{fi,c}(t)$ to be input to the voltage flicker algorithm to generate the flicker emission value. Oversampling ratios should be different every 2-cycle window to get a final fixed sampling rate. The system architecture becomes more complicated. Therefore, we propose to generate $u_o(t)$ at a fixed sampling rate (6.4kHz is the selected rate in our implementation) and apply a classical downsampling to get a new data stream suitable for the flicker algorithm (400 Hz in our implementation).

5. Laboratory test

To test our implementation of power quality procedures meeting the IEC 61400-21 standard, two laboratory setups have been used. Results are shown for the first test. It consists of a 110 V wounded-rotor induction motor coupled to a synchronous generator via an elastic torque transducer as shown in Figure 5. The synchronous generator supplies the necessary load to simulate the power curve of a wind turbine.

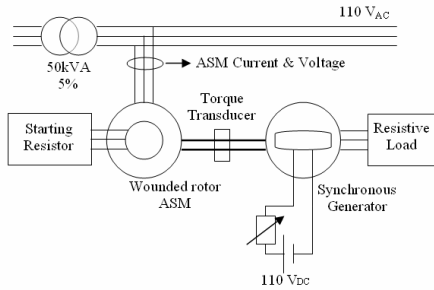


Fig. 5: Schematic of laboratory setup.

Shaft asymmetries ensure the presence of modulated currents at terminals as it is shown in Figure 6.

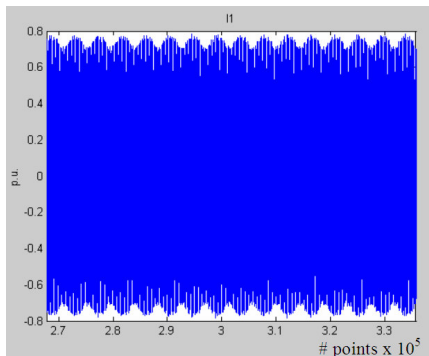


Fig. 6: $I(t)$ in per-unit at a wind speed of 5.5m/s.

The generation of the ideal voltage $u_o(t)$ is correctly performed and it fulfills the desired properties: same phase as the measured voltage and no perturbations. A detail is plotted in Figure 7.

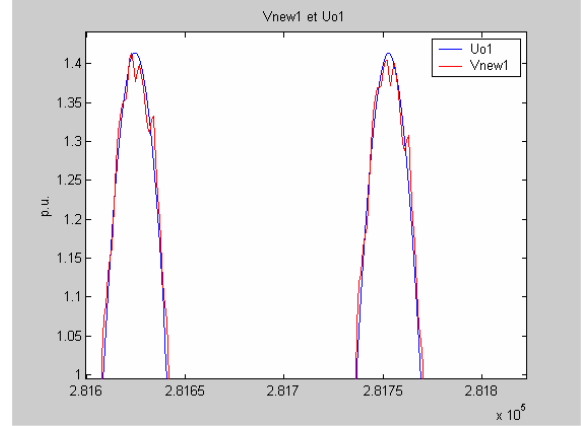


Fig. 7: Signals superposition, $u_o(t)$ and $V_{new}(t)$

After normalization and weighting processes, and depending on the network impedance phase angle ψ_k and the annual average wind speed v_a , the 99% percentile of the values in the wind speed interval from cut-in to 15m/s are reported as an output of the algorithm. Flicker coefficients $c(\psi_k, v_a)$ are shown in Table 1 for continuous operation of the asynchronous motor.

Table 1: Flicker coefficients.

v_a	6 m/s	7.5 m/s	8.5 m/s	10 m/s
ψ_k				
30°	3.9978	4.0929	4.2876	4.5912
50°	3.9978	4.0929	4.2876	4.6029
70°	4.0574	4.0937	4.3344	4.6029
85°	4.0574	4.0937	4.3344	4.6029

The assessment that follows is a fairly simple procedure and it specifies how the reported flicker coefficients can be used to estimate the flicker emission from a single wind turbine or a group of wind turbines operating continuously on any specific site. Equation (2) applies. P_{st} values are calculated for the short circuit power of the installation. Short circuit impedance value and angle are obtained from the power transformer feeding the asynchronous motor:

$$\left. \begin{array}{l} S_{TFO} = 50kVA \\ S_{MAS} = 11.432 kVA \end{array} \right\} \Rightarrow \begin{cases} S_{TFO}^{pu} = 1 pu \\ S_{MAS}^{pu} = 0.23 pu \\ S_{cc}^{pu} = \frac{1}{0.05} = 20 pu \end{cases} \quad (8)$$

The short circuit ratio is given by :

$$\frac{S_{CCréseau}}{S_{nMAS}} = 86.95 \quad (9)$$

The obtained results are shown in figures 8 and 9, where the measured P_{st} contribution is plotted versus wind speed set points (Figure 8) and versus active power (Figure 9).

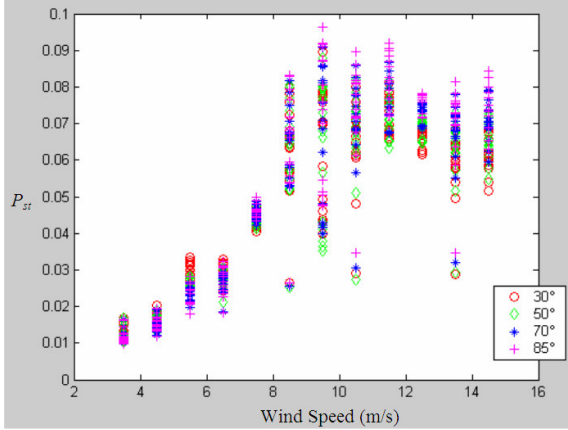


Fig. 8: P_{st} level on the 110V grid from data acquisition system vs. wind speed for 30°, 50°, 70° and 85° grid impedance angle.

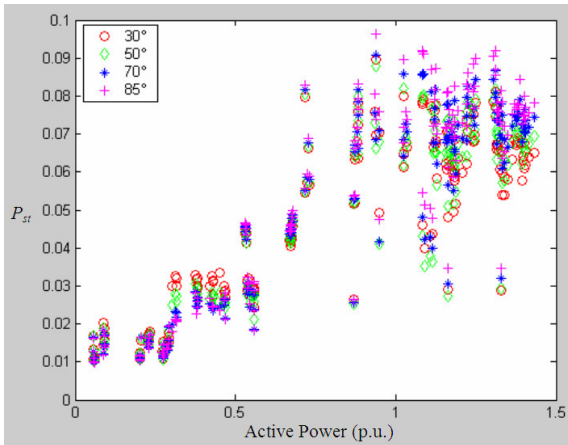


Fig. 9 P_{st} level on the 110V grid from data acquisition system vs. active power for 30°, 50°, 70° and 85° grid impedance angle.

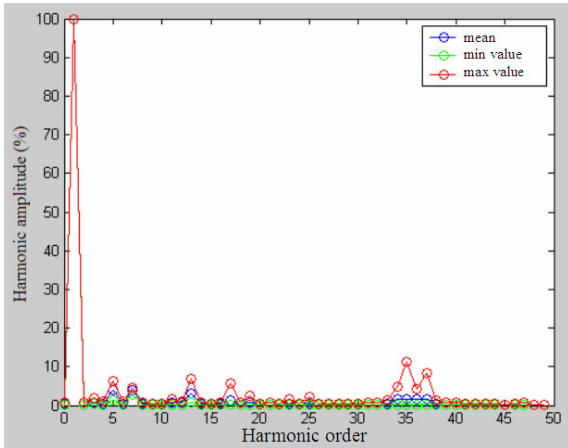


Fig. 10: Mean values of harmonic currents in percent of rated current.

The harmonic content of the current is also computed and presented in Figure 10, where the mean values in per cent at rated current is plotted.

6. Future work

The second laboratory setup aims at evaluating the flicker emission when several wind turbines are connected at the PCC. Three motor banks of similar characteristics as the one utilized during the first laboratory test are available. We wish to evaluate the influence of simulated wind speed, and number of motors operating in parallel on the flicker emission level.

Previous work by the authors comprised the development of a prototype for measuring the harmonic source impedance seen from the PCC of a Thevenin equivalent [6]. The network equivalent is represented in Figure 11 as seen from the coupling point of a wind farm. The source impedance value Z_{sh} gives us a measure of the true harmonic emission level, since this impedance represents an accurate image of the network characteristics. The product Z_{sh} by generated wind current I_h constitutes the real emission from the wind power production. The responsibility of the network is estimated from the open-circuit voltage E_{sh} .

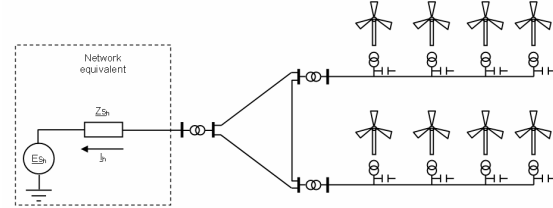


Fig. 11: Network Thevenin equivalent.

It is not the aim of this work to discuss the actual methodology in use for coefficient estimation during the measurement procedure proposed by the standard, but to propose an improvement regarding the second phase of power quality assessment once the wind turbine is connected at the PCC by the realization of an on-line source impedance measurement.

Nowadays, grid angle dependability is considered by selecting the right coefficient from manufacturer's data. Generally, the short-circuit power is calculated. The nature and the accuracy of data to be provided for modelling the network are not always evaluated in the same way. Besides, the source impedance is a time-dependent parameter, varying with a change of network topology, as for example the connection or disconnection of a second parallel transmission line or a second transformer at the bus bar. The development of dispersed generation will lead to important short-circuit level variations as well.

We propose to consider apparent short-circuit power variations of the real grid, by evaluating both the fundamental and harmonic source impedance value and its angle. This possibility gives rise to new challenges on the voltage fluctuation assessment, such as more accurate grid-dependent on-line estimation of flicker emission levels. The influence of other fluctuating generators or loads that may cause significant voltage variations at the wind turbine terminals could then be identified and responsibilities assigned. The final step in this project is to compare both methods of evaluating the flicker contribution. The assessment of the grid impedance will allow not only assigning responsibilities but will also facilitate the design of equipment, network components, tuning of control systems and protection configuration. The development of dispersed generation will be positively influenced by the capacity of measuring the network strength.

7. Conclusions

IEC defines a method based on voltage and current measurement to evaluate power quality characteristics, independent of the grid where the wind turbine is connected. The proposed algorithm has been implemented and tested, and it performs well. A high accuracy is obtained during the simulation procedure thanks to a software resampling algorithm in spite of the constant sampling rate originally set during data acquisition.

The measured power quality characteristics can thus be applied to calculate the influence on the voltage quality on another site given by its short circuit power and its impedance angle.

References

- [1] IEC-61400-21, "Wind Turbines, Part 21: Measurement and assessment of power quality characteristics of grid connected wind turbines".
- [2] P. Sørensen and al, "European Wind Turbine Testing Procedure Developments. Task 2: Power Quality", Riso National Laboratory, May 2001.
- [3] T. Thiringer, T. Petru and S. Lundberg: "Flicker contribution from wind turbine installations", IEEE Transactions on Energy Conversion, Vol. 19, No. 1, March 2004.
- [4] O. Gonbeau, L. Berthet, J. L. Javerzac, "Method to determine contribution of the customer and the power system to the harmonic disturbance", CIRED, Barcelona, Spain, 12-15 May 2003.
- [5] X. Robe, "Introducing power quality monitoring functions in digital protective relays", DEA at the ULB, Electrical Engineering Department, 2002.
- [6] A. Morales and J.C. Maun: "Power quality responsibilities by grid impedance assessment at a wind power production", CIRED, Barcelona, Spain, 12-15 May 2003.